The Effects of PDFs on the Line-to-Line Voltage and Noise Generated by PWM Inverters

Khalid Ali Almarri Juan Carlos Balda

Department of Electrical Engineering
University of Arkansas
3217 Bell Engineering Center
Fayetteville, AR 72701
(501) 575-6578

Abstract *- Acoustic noise is a drawback of PulseWidth Modulated (PWM) inverters switching at frequencies within the audible range. This drawback becomes an important concern when the PWM inverter is located in the vicinity of people (e.g., industrial sites, HVAC installations, etc.). Increasing the switching frequency beyond the audible range is a possible solution that unfortunately leads to the derating of the PWM inverter. On the other hand, random PWM techniques are economical alternatives for acoustic noise reduction. To this end, this paper firstly addresses the development of a random space vector PWM algorithm making use of a small number of switching frequencies (i.e., a limited pool). The random PWM algorithm controls the speed of an induction motor (IM) driven under the constant V/Hz principle. Then, this paper compares the impact that different well-known Probability Density Functions (PDFs) assigned to the switching frequencies in the limited pool have upon the line-to-line voltage waveform and acoustic noise. The PDFs are implemented in a TI TMS320C240 fixed-point digital signal processor (DSP) that is used to control a three-phase IM.*

I. INTRODUCTION

PWM waveforms having a fixed switching frequency are composed of a component at the desired fundamental frequency and a number of harmonic clusters centered at each integer multiple of the switching frequency [1]. These harmonic clusters are a direct source of the acoustic noise, which is an objectionable issue for PWM inverters placed in the vicinity of people. Random PulseWidth Modulation (RPWM) techniques have emerged as the most favorable approach for acoustic noise reduction in AC drives [2-6]. These techniques pseudo-randomly vary the length of successive switching periods (or the instantaneous switching frequency) within a specified switching range causing the harmonic clusters to spread over the spectral range. The number of used switching frequencies is usually as high as the maximum number that can be practically implemented within the desired switching range using a DSP.

Recently, a study proposed to limit the number of switching frequencies to five or six (i.e., a limited pool) [7]. An off-line selection procedure called Common-Multiple Deviation (CMD) scans for the best switching frequencies using the following equation:

$$d(f) = \sqrt{\frac{1}{N}\sum_{i=1}^{N}\left[\frac{f}{f_i} - round\left(\frac{f}{f_i}\right)\right]^2} \qquad (1)$$

where f denotes the spectral frequency, f_i (i = 1, 2, ..., N) represents the different switching frequencies in the pool, and round(•) denotes the closest integer. Each switching frequency is selected so its harmonics over the considered spectral range are not close to any common multiple of the switching frequencies in the pool. In this paper, the considered spectral range is 20 kHz, the number of the switching frequencies in the pool (N) is 5, and the switching frequencies were limited to the 3.5 – 7.5 kHz range.

The best five switching frequencies selected by the CMD method were 3676, 4664, 5733, 6443, 7267 Hz. A comparison between the line-to-line voltage spectra at the fixed switching frequency of 5 kHz and the limited-pool RPWM using an uniform PDF is shown in Figure 1. This figure clearly illustrates the advantages of RPWM where the peak of the harmonic cluster was reduced approximately 84% (Figure 1 (b)) when compared to the one of the fixed-switching-frequency PWM (Figure 1 (a)).

This paper firstly addresses the development of a RPWM technique in the TMS320C240 DSP. Secondly, it evaluates the effects that different well-known PDFs assigned to the switching frequencies in the above limited pool have upon the line-to-line voltage spectrum and the acoustic noise generated by an IM controlled by a TI TMS320C240 DSP. Measured results provide the foundations for the analysis presented in this paper.

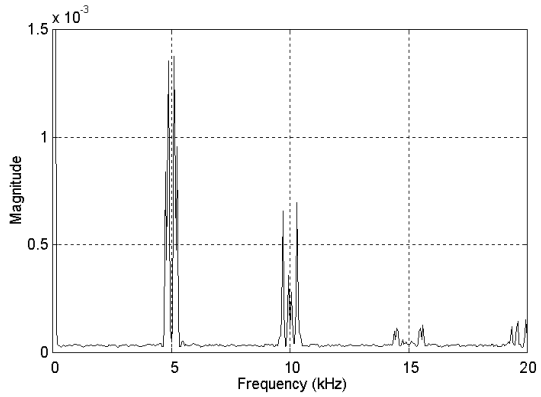

(a)

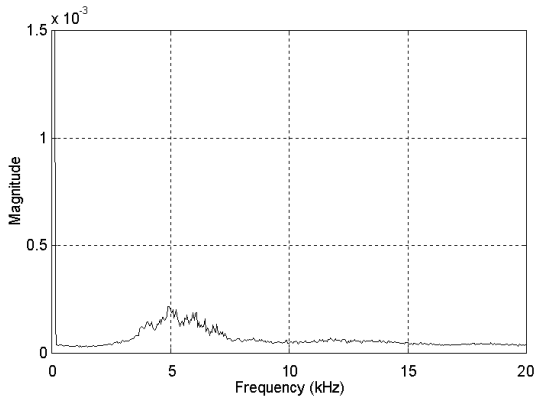

(b)

Figure 1 Line-to-line voltage spectrum:
(a) fixed-switching-frequency PWM,
(b) limited-pool RPWM.

II. IMPLEMENTATION OF RPWM ON THE TMS320C240 DSP

Space Vector PWM (SVPWM) designates a series of switching patterns of three controlling signals "abc" fed to a PWM inverter. These signals are based on the notion of approximating a (commanded voltage) vector U_{out} in a two-dimensional stationary reference frame [8]. The vector U_{out} can be "regenerated" using stationary (voltage) vectors that are adjacent and 60° apart from each other as shown in Figure 2. A typical switching sequence of the controlling signals for U_{out} located in the first sector is shown in Figure 3. The time intervals T_1, T_2, and T_n can be calculated as follows [8]:

$$T_1 = M \cdot T_{sw} \cdot \sin(60 - \alpha)$$
$$T_2 = M \cdot T_{sw} \cdot \sin \bullet$$
$$T_n = T_{sw} - T_1 - T_2$$

where M is the modulation index, T_{sw} is the instantaneous switching period (i.e., $1/f_{sw}$ where f_{sw} is the instantaneous switching frequency) and α is the angle between the rotating vector U_{out} and its adjacent vector in the clockwise direction.

The limited-pool RPWM techniques pseudo-randomly alternate the successive switching periods T_{sw} between the (five) switching frequencies available in the limited pool. Hence, the main differences between these techniques are in the method used to pseudo-randomly vary the successive switching periods and the number of switching frequencies in the pool.

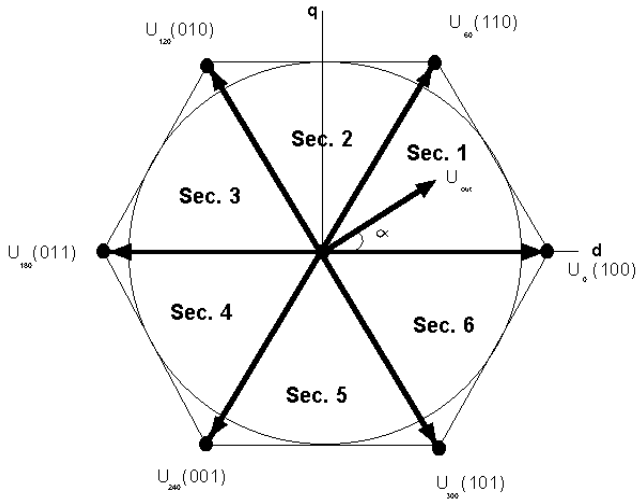

Figure 2 Space vectors in the stationary d-q plane.

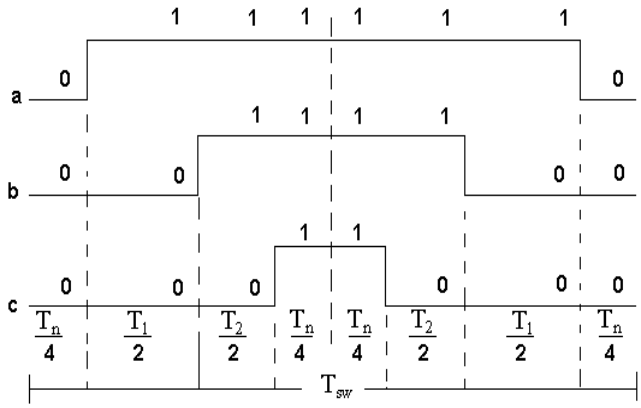

Figure 3 Typical SVPWM modulation sequence.

The implementation of the RPWM in the TMS320C40 DSP was based on the SVPWM technique given in the TI Application Report SPRA284 [9]. The DSP code was modified and reconfigured to operate in the random mode by taking advantage of the on-the-fly change feature. The timer-compare and period registers have shadow registers. This feature allows the application code to update the timer-compare and period registers in order to change the timer

period and the width of the pulse for the following period while the current period is still in progress.

Five different values of the period register (corresponding to the switching frequencies in the pool) were calculated off-line using (2) and stored in the DSP memory.

$$Period\_R = \frac{1}{f_{sw} \times 2 \times 50 \times 10^{-9}} \tag{2}$$

For each switching cycle, one period is selected randomly using an on-line linear congruential generator and fed to the shadow registers of the timer-compare and period registers to be used in the next cycle.

III. EXPERIMENTAL SETUP

A diagram of the experimental setup is depicted in Figure 4. A TI TMS320C240 fixed-point DSP controls a two-level voltage-source inverter through an operator interface board. The inverter is driving an unloaded 208-V, 1-hp, 4-pole, three-phase IM. The amplified signal from a microphone and the line-to-line voltage signal (measured with high-voltage differential probe and a Tektronix A6902B voltage isolator) are fed to a Tektronix 2630 Fourier Analyzer. The microphone is placed at a distance of one meter from the IM. The Fourier Analyzer was configured to use a Hanning window with a frame size of 1024 and an averaging process of 200 times. The analyzer data is then sent to a PC for analyses and plotting.

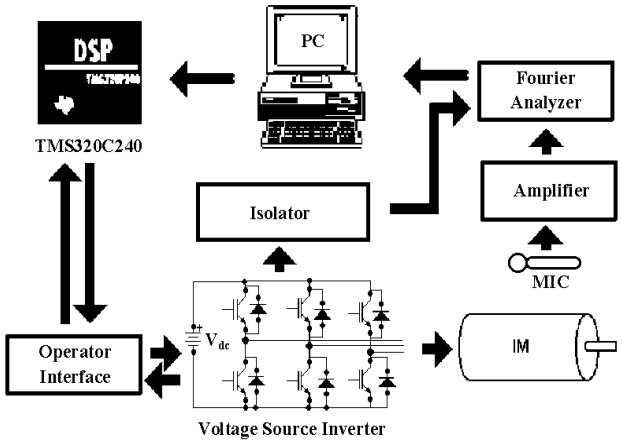

Figure 4 Experimental setup.

IV. MEASURED RESULTS FOR VARIOUS PDFS

Seven well-known PDFs in addition to one arbitrary PDF (see Table 1) are examined in this paper. Since the pool has a limited number of switching frequencies, the probability of these frequencies for all considered PDFs could be calculated using:

$$p_{l\_p}(f_i) = \frac{p(f_i)}{\sum_{i=1}^{N} p(f_i)} \tag{3}$$

The probabilities of the switching frequencies in the limited pool for all considered PDFs are tabulated in Table 1. The remainder of this section presents the measured results for all eight PDFs. A comparison of the results is performed in the next section.

TABLE 1
THE PROBABILITIES OF THE SWITCHING FREQUENCIES IN THE LIMITED POOL FOR ALL CONSIDERED PDFS.

PDF	$P_{l\_p}(f_1)$	$P_{l\_p}(f_2)$	$P_{l\_p}(f_3)$	$P_{l\_p}(f_4)$	$P_{l\_p}(f_5)$
Uniform	0.2	0.2	0.2	0.2	0.2
Trapezium	0.1323	0.1679	0.2063	0.2319	0.2616
Pink hyperbolic	0.2852	0.2248	0.1829	0.1627	0.1443
Laplacian	0.2741	0.2290	0.1886	0.1657	0.1427
Cauchy	0.2724	0.2292	0.1888	0.1661	0.1434
Rayleigh	0.1860	0.2060	0.2107	0.2053	0.1921
Maxwell	0.1726	0.2117	0.2215	0.2102	0.1841
Arbitrary	0.2460	0.1563	0.0977	0.2070	0.2930

1. Uniform PDF:

The uniform PDF is given by:

$$p(f) = \frac{1}{f_{\max} - f_{\min}} \tag{4}$$

Plots of the uniform PDF, the measured voltage spectra and noise are shown in Figures 5 – 7, respectively.

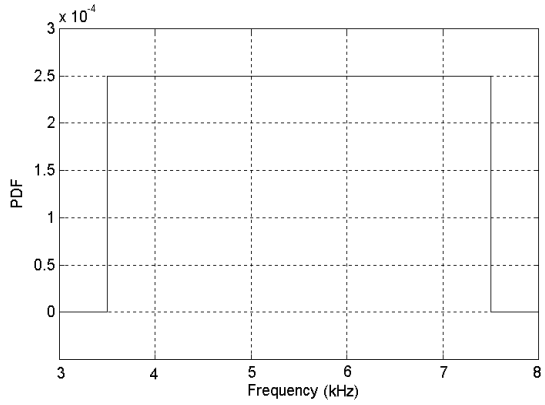

Figure 5 Uniform PDF.

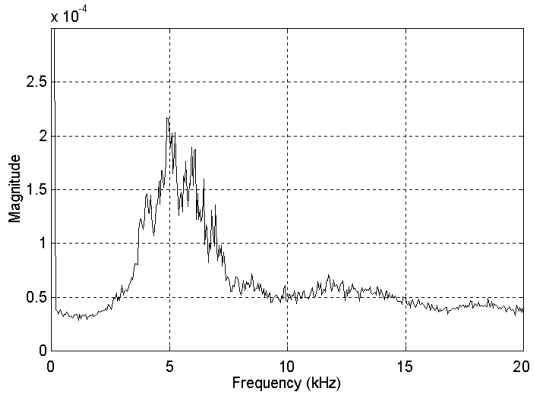

Figure 6 Uniform PDF line-to-line voltage spectrum.

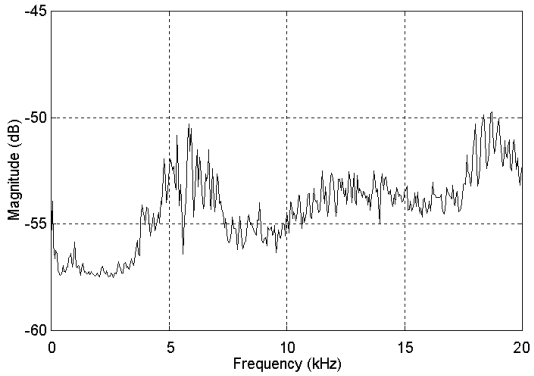

Figure 7 Uniform PDF noise spectrum.

2. Trapezium PDF:

The trapezium PDF is given by:

$$p(f) = \frac{2f}{f_{\max}^2 - f_{\min}^2} \tag{5}$$

A plot of the trapezium PDF is depicted in Figure 8, the probability linearly increases by increasing the frequency. This produces a higher average switching frequency when compared to the uniform PDF. Plots of the measured voltage and noise spectra are shown in Figures 9 and 10, respectively.

3. Pink hyperbolic PDF:

Another well-known PDF is the Pink hyperbolic PDF, which is characterized by the higher probability of the lower frequencies causing the average switching frequency to be less than the center frequency of the switching range. The mathematical function of this PDF is governed by:

$$p(f) = \frac{1}{\left(\log f_{\max} - \log f_{\min}\right) f} \tag{6}$$

Plots of the Pink hyperbolic PDF, the measured voltage and noise spectra are shown in Figures 11 – 13, respectively.

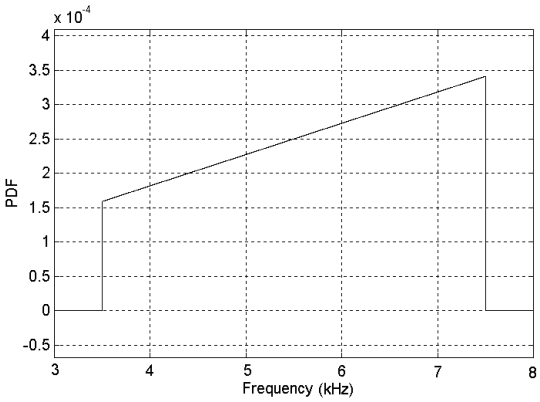

Figure 8 Trapezium PDF.

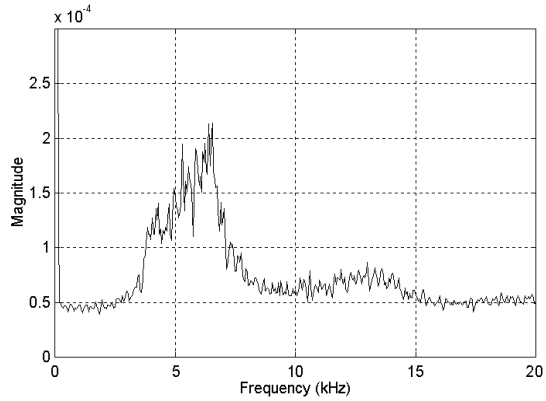

Figure 9 Trapezium PDF line-to-line voltage spectrum.

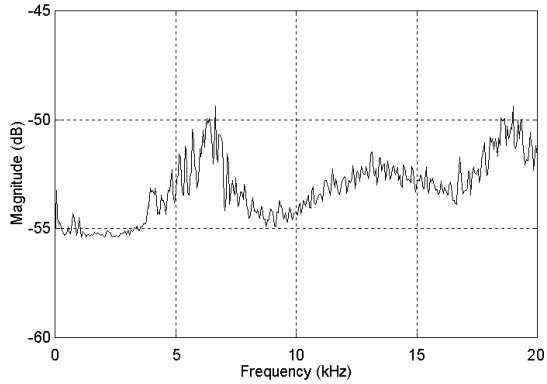

Figure 10 Trapezium PDF noise spectrum.

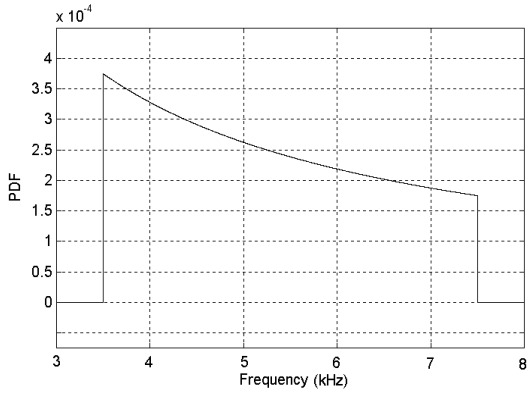

Figure 11 Pink hyperbolic PDF.

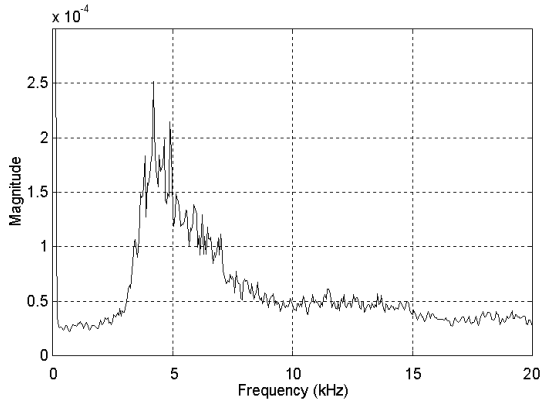

Figure 12 Pink hyperbolic PDF line-to-line voltage spectrum.

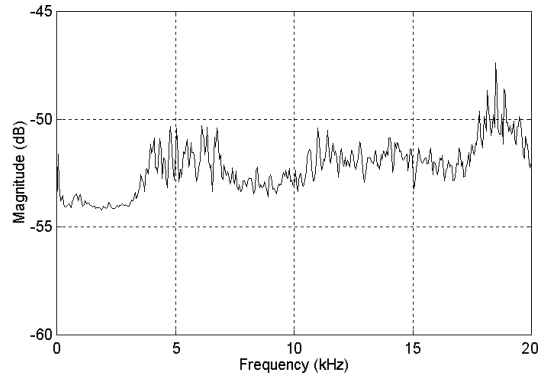

Figure 13 Pink hyperbolic PDF noise spectrum.

4. Laplacian PDF:

The Laplacian PDF is given by:

$$p(f) = \frac{\alpha}{2} e^{-\alpha|f|} \qquad , \alpha = 1/5500 \tag{7}$$

where α is $2/(f_{min} + f_{max})$. Plots of the Laplacian PDF, the measured voltage and noise illustrated are shown in Figures 14 – 16, respectively.

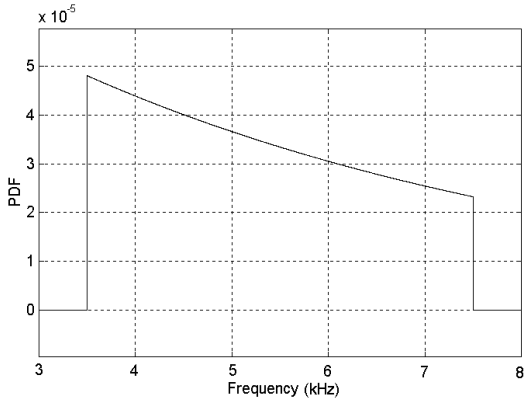

Figure 14 Laplacian PDF.

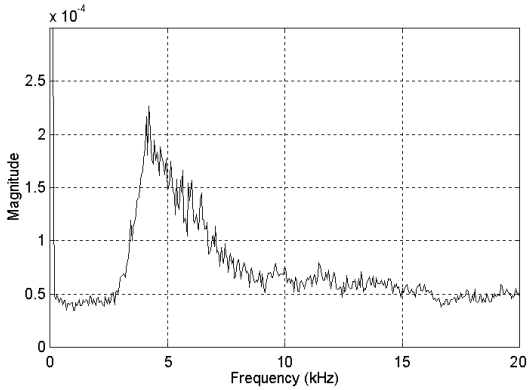

Figure 15 Laplacian PDF line-to-line voltage spectrum.

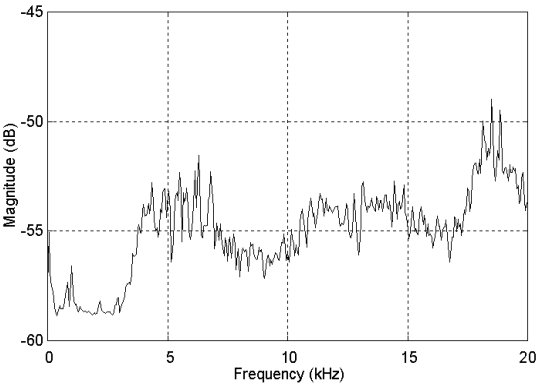

Figure 16 Laplacian PDF noise spectrum.

5. Cauchy PDF:

The Cauchy PDF is similar to the Laplacian PDF. Its mathematical function is given by:

$$p(f) = \frac{\alpha}{\pi\left(\alpha^2 + f^2\right)} \quad , \alpha = 5500 \qquad (8)$$

where α is $(f_{min} + f_{max})/2$. Plots of the Cauchy PDF, the measured voltage and noise spectra are depicted in Figures 17 – 19, respectively.

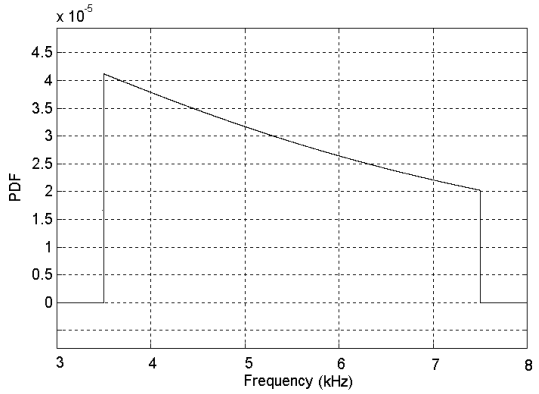

Figure 17 Cauchy PDF.

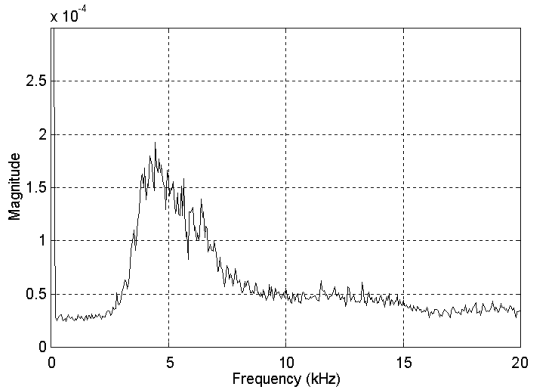

Figure 18 Cauchy PDF line-to-line voltage spectrum.

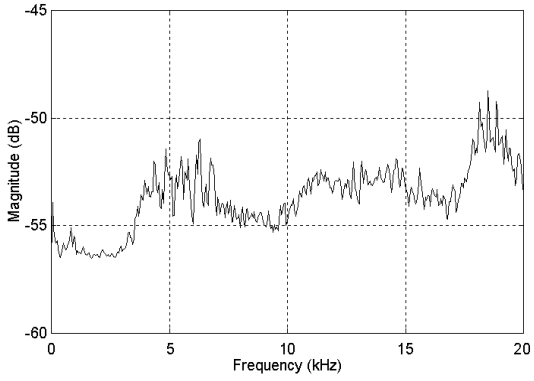

Figure 19 Cauchy noise spectrum.

6. Rayleigh PDF:

The Rayleigh PDF is similar to the normal (Gaussian) PDF with the exception that the right side probability decreases at a slower rate than the left side probability shifting the average switching frequency to higher part of the switching range. The mathematical function of this PDF is given by:

$$p(f) = \frac{f}{\alpha^2} e^{-\frac{f^2}{2\alpha^2}} \quad , \qquad \alpha = 5500 \qquad (9)$$

where α is $(f_{min} + f_{max})/2$. Plots of the continuous PDF, the measured voltage and noise spectra are shown in Figures 20 – 22, respectively.

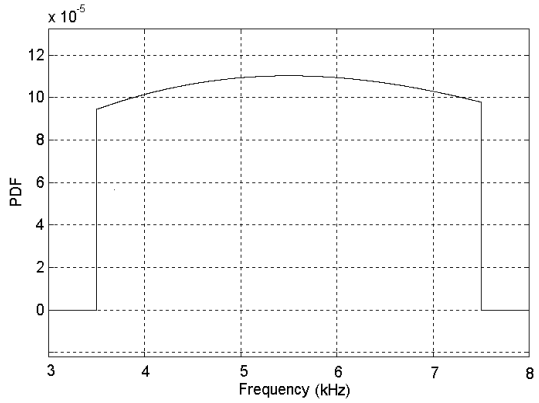

Figure 20 Rayleigh PDF.

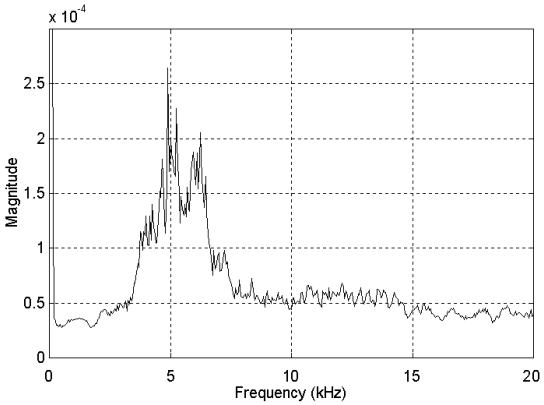

Figure 21 Rayleigh PDF line-to-line voltage spectrum.

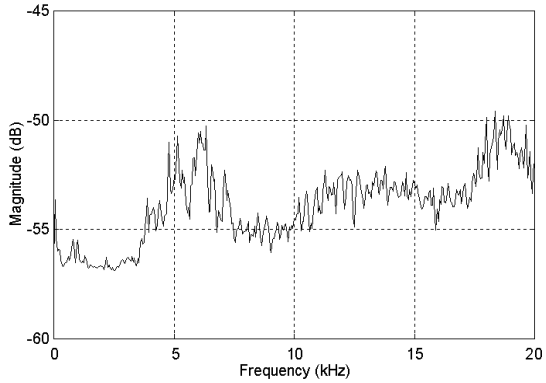

Figure 22 Rayleigh PDF noise spectrum.

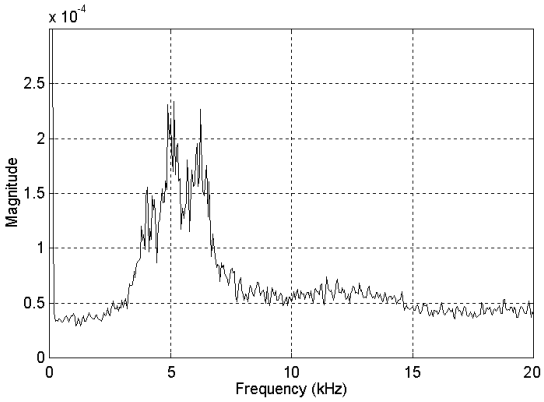

Figure 24 Maxwell PDF line-to-line voltage spectrum.

7. Maxwell PDF:

The Maxwell PDF is also similar to the Rayleigh PDF having a slower probability variation rate of the frequencies. Its mathematical function is given by:

$$p(f) = \frac{\sqrt{2}}{\alpha^3\sqrt{\pi}} f^2 e^{-\frac{f^2}{2\alpha^2}} \quad , \alpha = 3889 \qquad (10)$$

where α is $(f_{min} + f_{max})/(2\sqrt{2})$. Plots of the Maxwell PDF, the measured voltage and noise spectra are given in Figures 23 – 25, respectively.

8. Arbitrary-selected PDF:

The selection of the probabilities for the five switching frequencies was done by observing first the line-to-line voltage spectrum of the uniform PDF, and then trying to assign some values so the spectrum would be flatter. The values of the assigned probabilities are shown in Table 1. The resultant line-to-line voltage spectrum and the noise spectrum are shown in Figures 26 and 27, respectively.

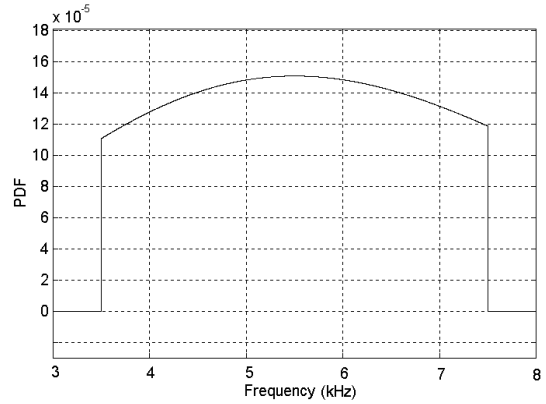

Figure 23 Maxwell PDF.

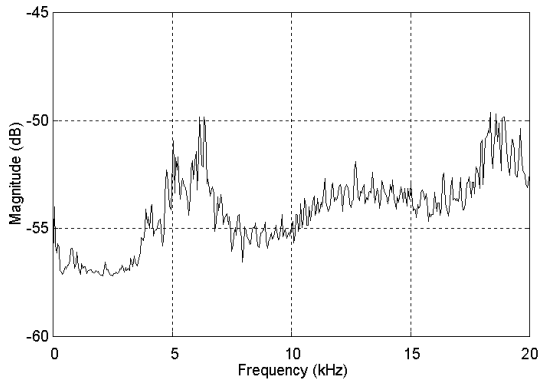

Figure 25 Maxwell PDF noise spectrum.

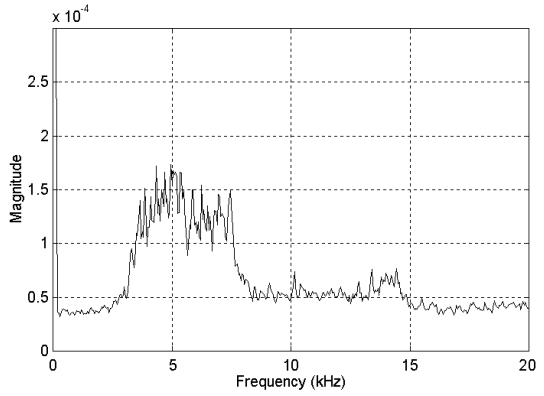

Figure 26 Arbitrary-selected line-to-line voltage spectrum.

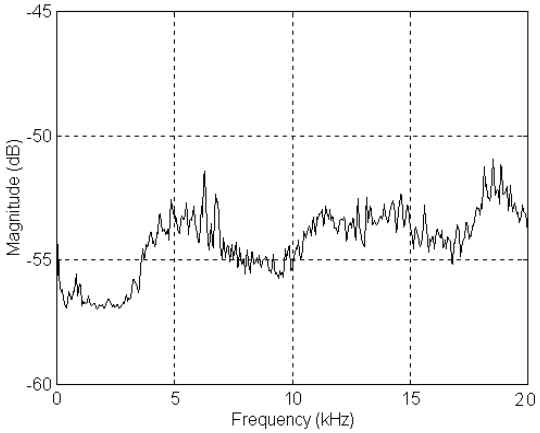

Figure 27 Arbitrary-selected noise spectrum.

V. ANALYSIS AND CONCLUSIONS

The above results indicate that the line-to-line voltage spectrum takes a similar shape to that of the PDF within the switching-frequency range. This is also reflected on the noise spectrum suggesting that the line-to-line voltage spectrum has a direct impact on the acoustic noise spectrum. These measured effects imply that there is a pseudo-linear relation between the PDF and the line-to-line voltage spectrum given that the pool of switching frequencies is small. The theory and development of this pseudo-linear relationship is out of the scope of this paper.

Only the arbitrary selected PDF seems to produce flatter spectra with measured lower peaks. Table 2 compares the peaks of both the line-to-line voltage and noise spectra of all PDFs to the arbitrary-selected PDF. The first column shows the percentage increase of the maximum peak of the line-to-line voltage spectrum for the considered PDF with respect to the maximum peak of the arbitrary-selected PDF. The second column illustrates the (dB) increase of the maximum peak of the noise spectrum for the considered PDF over the maximum peak of the arbitrary-selected PDF. None of the considered PDFs reduces the acoustic noise than the others.

TABLE 2
THE MAXIMUM PEAKS OF THE SEVEN PDFS COMPARED TO THE MAXIMUM PEAK OF THE ARBITRARY-SELECTED PDF.

PDF	peak increase of $V_{l\text{-}l}$ spectrum (%)	peak increase of the noise spectrum (dB)
Uniform	24.89	2.218
Trapezium	23.15	2.257
Pink hyperbolic	45.19	4.552
Laplacian	30.73	2.943
Cauchy	11.15	3.203
Rayleigh	52.24	2.346
Maxwell	34.96	2.311

For example, the Cauchy PDF has the second lowest increase of the voltage peak but it has the third highest increase of the noise peak. In conclusion, there are opportunities for future work leading to an optimized selection of the probabilities of the switching frequencies in a limited pool.

REFERENCES

[1] J. T. Boys and P. G. Handly, "Harmonic analysis of space vector modulated PWM waveforms", *IEE Proceedings Part B*, Volume 137, No. 4, pp. 197-204, 1990.

[2] J. T. Boys and P. G. Handly, "Spread spectrum switching: Low noise modulation technique for PWM inverter drives", *IEE Proceedings Part B*, Volume 139, No. 3, pp. 252-260, May 1992.

[3] T. G. Habetler and D. M. Divan, "Acoustic noise reduction in sinusoidal PWM drives using a random modulation carrier", *IEEE Transactions on Power Electronics*, Volume 6, No. 3, pp. 356-365, July 1991.

[4] J. T. Boys, "Theoretical spectra for narrow-band random PWM waveform", *IEE Proceedings Part B*, Volume 140, No. 6, pp. 393-400, Nov. 1993.

[5] A. M. Trzynadlowski, F. Blaabjerg, J. K. Pedersen, R. L. Kirlin and S. Legowski, "Random pulse width modulation techniques for converter-fed drive systems – A review", *IEEE Transactions on Industry Applications*, Volume 30, No. 5, pp. 1166-1175, Sept./Oct. 1994.

[6] G. A. Covic and J. T. Boys, "Noise quieting with random PWM AC drives", *IEE Proceedings Part B*, Volume 145, No. 1, pp. 1-10, Jan. 1998.

[7] A. M. Trzynadlowski, M.M. Bech, F. Blaabjerg, J. K. Pedersen, R. L. Kirlin and M. Zigliotto, "Optimization of switching frequencies in the limited-pool random space vector PWM technique for inverter-fed drives", *1999 Applied Power Electronics Conference (APEC '99)*, Dallas (TX), pp. 1013-1018, March 14-18, 1999.

[8] A. M. Trzynadlowski; *The Field Orientation Principle in Control of Induction Motors*, Kluwer Academic Publishers, Massachusetts, 1994.

[9] Z. Yu and D. Figoli, "Using constant V/Hz principle and space vector PWM technique for AC induction motor control with TMS320C240", *Application Report SPRA284, Texas Instruments*, Dec. 1997.